Dynamics of matter solitons in weakly modulated optical lattices

V. A. Brazhnyi,[1,*] V. V. Konotop,[1,2,†] and V. Kuzmiak[3,‡]
[1]*Centro de Física Teórica e Computacional, Universidade de Lisboa, Complexo Interdisciplinar, Avenida Professor Gama Pinto 2, Lisbon 1649-003, Portugal*
[2]*Departamento de Física, Universidade de Lisboa, Campo Grande, Edificio C8, Piso 6, Lisboa 1749-016, Portugal*
[3]*Institute of Radio Engineering and Electronics, Czech Academy of Sciences, Chaberska 57, 182 51 Prague 8, Czech Republic*
(Received 16 February 2004; revised manuscript received 22 April 2004; published 5 October 2004)

It is shown that matter solitons can be effectively managed by means of smooth variations of parameters of optical lattices in which the condensate is loaded. The phenomenon is based on the effect of lattice modulations on the carrier wave transporting the soliton and that is why it is well understood in terms of the effective mass approach, where a particular spatial configuration of the band structure is of primary importance. Linear, parabolic, and spatially localized modulations are considered as case examples. It is shown that these defects can originate an accelerating and oscillating motion of matter solitons as well as they can simulate soliton interactions with attractive and repulsive defects.

DOI: 10.1103/PhysRevA.70.043604 PACS number(s): 03.75.Lm

I. INTRODUCTION

The realization of a Bose-Einstein condensate (BEC) in an optical lattice [1] originated intensive experimental and theoretical studies [1–14] of the phenomenon. One of the main features induced by the periodicity is the appearance of a band structure in the spectrum of the underlying linear system, i.e., the gas of noninteracting atoms. The band spectrum is responsible for a number of effects, including modulation instability [3,4] and formation of gap solitons [4], Landau-Zener tunneling [5,6], Bloch oscillations of BEC's [1,5,7], the lensing effect [8], soliton stabilization [9], etc. These effects, being based on the properties of the linear system, are well described in terms of the concept of the effective mass, which takes into account the wave nature of the phenomenon and that is why its inverse value is also referred to as the group velocity dispersion [4]. In practice, laser lattices are never perfect. In particular, they are often imposed simultaneously with other external potentials, like, for example, a magnetic trap which significantly affects the motion of a soliton [10]. Moreover, one can create spatially localized lattices; propagation of matter waves through these displays a number of interesting properties [11] such as resonant transmission and soliton generation through modulational instability. It is also highly relevant to mention that very recently direct experimental observation of a gap matter soliton in an ^{87}Rb BEC, containing about 250 atoms, has been reported [12].

In this paper we present an analysis of the BEC dynamics in an optical lattice with smoothly modulated parameters. In this case the band gap structure is still preserved but is deformed by the modulation. In particular, we show that this is a way of managing the dynamics of matter waves—making them accelerating, oscillating, etc.

The model and the physics of the phenomenon are described in Sec. II. Acceleration of a matter soliton in a linearly modulated lattice is considered in Sec. III. Soliton oscillations in a lattice with a parabolic modulation of the depth are considered in Sec. IV. Section V is devoted to soliton interaction with spatially localized defects. The results of the paper are summarized in the Conclusion.

II. PHYSICS OF THE PHENOMENON

Let us consider a trap potential which can be written down in the form $V_{trap}=(m/2)(\omega_{\|}^2x^2+\omega_0^2y^2+\omega_0^2z^2)+V_{\epsilon}(x)$. The first term in the right hand side of this expression describes a magnetic trap with $\omega_{\|}$ and ω_0 being the longitudinal and transverse linear oscillator frequencies. The condensate is chosen to have a cigar shape with the aspect ratio satisfying the relation $\omega_{\|}/\omega_0 \ll a_0^2/\xi^2 \ll 1$ (a_0 and ξ being the transverse linear oscillator length and the healing length, respectively). We are interested in excitations of a BEC having characteristic scales of order of the healing length and a relatively small potential amplitude, which allows us to neglect the term $(m/2)\omega_{\|}^2x^2$ in the expression for the trap potential V_{trap}. The term $V_{\epsilon}(x)$, where ϵ is a deformation parameter controlling the potential shape, describes a smoothly modulated optical lattice. It will be assumed to have the form $V_{\epsilon}(x)\equiv f(\epsilon^{3/2}x)V_0(x)$, where $V_0(x)=V_0(x+L)$ is the unperturbed lattice having period L of order of the linear oscillator length a_0, $L\sim a_0$, and $f(\epsilon^{3/2}x)$ is a smooth modulation normalized as follows: $f(0)=1$. Smoothness in the present context means slow variation of $f(\epsilon^{3/2}x)$ on the scale of the healing length, or in other words $\epsilon\sim a_0/\xi$. Then one can apply a multiple-scale expansion [4] in order to reduce the Gross-Pitaevskii equation governing the dynamics of the BEC to an effectively one-dimensional (1D) nonlinear Schrödinger (NLS) equation with a slowly varying effective mass $m_{\alpha}\equiv m_{\alpha}(\epsilon^{1/2}X)=[\partial_k^2\mathcal{E}_{\alpha}(k;\epsilon^{1/2}X)]^{-1}$, and the group velocity of the carrier wave depending on the coordinate, $v_{\alpha}=\partial_kE_{\alpha}(k;\epsilon^{1/2}X)$:

*Electronic address: brazhnyi@cii.fc.ul.pt
†Electronic address: konotop@cii.fc.ul.pt
‡Electronic address: kuzmiak@ure.cas.cz

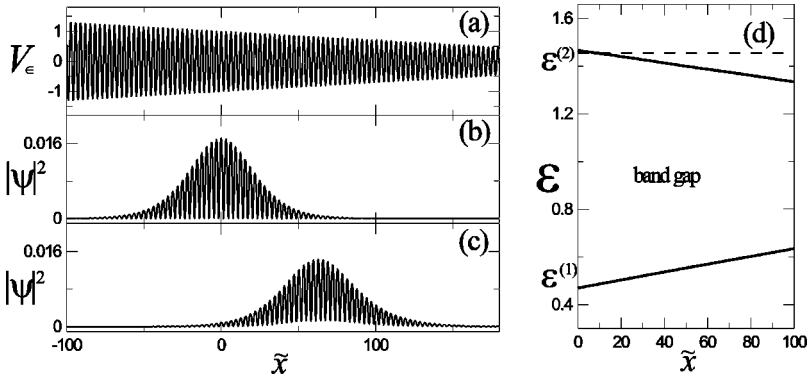

FIG. 1. (a) The linearly modulated periodic potential V_ϵ given by Eq. (7). (b) The initial profile of the condensate near the upper bound of the gap for $\mathcal{E}^{(2)}=1.46$. (c) The profile of the condensate at time $\tilde{t}=100$. (d) The band structure for the potential (7) (solid line) and the energy of the soliton (dashed line). All data are computed for $\epsilon=0.02$.

$$i\Psi_T + iv_\alpha\Psi_X = -(2m_\alpha)^{-1}\Psi_{XX} + \chi|\Psi|^2\Psi. \tag{1}$$

Hereafter, α and k stand for the number of the zone and for the dimensionless wave vector in the first Brillouin zone (BZ), respectively, $\chi=\mathrm{sgn}\, a_s$, a_s being the s-wave scattering length. In Eq. (1) we have passed to dimensionless slow variables: $X=\epsilon x/a_0=\epsilon\tilde{x}$ and $T=\epsilon^2\omega_0 t=\epsilon^2\tilde{t}$. Taking into account the smoothness of the potential, the spectrum $\mathcal{E}_\alpha(k;\epsilon^{3/2}\tilde{x})$ at some point of the space, say $\tilde{x}=\tilde{x}_0(\tilde{x}_0=x_0/a_0)$, can be computed from the linear eigenvalue problem

$$\frac{d^2\varphi_{\alpha k}}{d\tilde{x}^2} + [\mathcal{E}_\alpha(k;\epsilon^{3/2}\tilde{x}_0) - f(\epsilon^{3/2}\tilde{x}_0)V_0(\tilde{x})]\varphi_{\alpha k} = 0. \tag{2}$$

In order to get a qualitative picture of the effects that can be observed in the matter wave dynamics we carry out numerical simulations using the 1D model (justified for the low-density BEC's)

$$i\psi_{\tilde{t}} = -\psi_{\tilde{x}\tilde{x}} + f(\epsilon^{3/2}\tilde{x})V_0(\tilde{x})\psi + \chi|\psi|^2\psi. \tag{3}$$

It is to be emphasized here that ψ in Eq. (3) describes the complete macroscopic wave function whereas Ψ in Eq. (1) describes the behavior of its envelope.

In the case of a homogeneous lattice, i.e., Eq. (3) with $f(\tilde{x})\equiv 1$, there exists a solitary wave solution (bright matter soliton) which can be found by means of the stationary ansatz $\psi(\tilde{x},\tilde{t})=u(\tilde{x})e^{-i\mathcal{E}\tilde{t}}$, where $u(\tilde{x})$ is a real valued function satisfying the equation

$$u_{\tilde{x}\tilde{x}} + [\mathcal{E} - V_0(\tilde{x})]u - \chi u^3 = 0. \tag{4}$$

Let us consider now the boundary of the BZ, i.e., $|k_0|=\pi a_0/L$. As is known (see, e.g., [13]) stationary solitary wave solutions subject to zero boundary conditions $\lim_{|\tilde{x}|\to\infty}u(\tilde{x},\tilde{t})=0$ exist only if $\mathcal{E}$ belongs to a gap of the spectrum of (2). For the sake of definiteness, below we deal with the first (lowest) forbidden gap, for which the lower and upper edges will be denoted as $\mathcal{E}^{(1)}$ and $\mathcal{E}^{(2)}$, respectively [see an example in Fig. 1(d)]. Thus the frequency of a static matter soliton must satisfy the condition $\mathcal{E}^{(1)}<\mathcal{E}<\mathcal{E}^{(2)}$. Then in the case $\chi=-1(\chi=1)$ a small amplitude bright matter soliton can be excited with energy inside the gap in the vicinity of the upper $\mathcal{E}^{(2)}$ (lower $\mathcal{E}^{(1)}$) band edge, respectively [4]. For the next consideration it is important to mention that envelope solitons can also exist for $\mathcal{E}>\mathcal{E}^{(2)}$ if $\chi=-1$, and at $\mathcal{E}<\mathcal{E}^{(1)}$ if $\chi=1$. These solitons are created against a moving carrier wave background (with $|k|\neq|k_0|$ and $v_\alpha\neq 0$), i.e., they move with the velocity v_α, and are described by the formula

$$\Psi_s(X,T) = \frac{\sqrt{-\chi m_\alpha}N\,\exp[(i/8)m_\alpha N^2 T]}{2\,\cosh\left\{\begin{array}{l}1\\ -m_\alpha N[X - X_0(T)]\\ 2\end{array}\right\}}, \tag{5}$$

with either $\chi=-1$, $\alpha=2$, and $m_2>0$, or $\chi=1$, $\alpha=1$, and $m_1<0$. $X_0(T)=-v_\alpha T$ is the coordinate of the soliton center and N is the normalized number of atoms,

$$N = \int_{-\infty}^{\infty}|\Psi|^2 dX. \tag{6}$$

Strictly speaking Eq. (5) is a solution of the unperturbed NLS Equation (1) with v_α and m_α constants. Since, however, the parameters are changing slowly in space, the simplified picture based on the analytic form (5) appears to be good enough for a qualitative understanding of various phenomena.

In what follows the consideration is restricted to the case $\chi=-1$ and we discuss the dynamics of small amplitude bright matter solitons near the upper edge of the first band gap $\mathcal{E}^{(2)}$.

III. MATTER WAVE ACCELERATION

We first consider linear modulation of the lattice amplitude [see Fig. 1(a)]

$$V_\epsilon(\tilde{x}) = (1 - \epsilon^{3/2}\tilde{x})\cos(2\tilde{x}), \tag{7}$$

whose lowest forbidden gap is shown in Fig. 1(d).

Let us assume that in the vicinity of the origin, i.e., near $\tilde{x}=0$, a bright static gap soliton with $v_2=0$ is created [see Fig. 1(b)]. Due to the nonzero extension of the soliton, it partially occupies the space where the soliton energy falls into the allowed band [see Fig. 1(d)] and thus corresponds to running linear waves. This is the reason for the soliton to start to move toward the region with a narrower gap, i.e., in the positive direction. Since it is assumed that in the leading approximation the energy of the soliton is conserved, the group velocity of the background increases and, therefore, the soliton velocity grows when the coordinate of the soliton center increases [Fig. 2(a)], which gives rise to soliton accel-

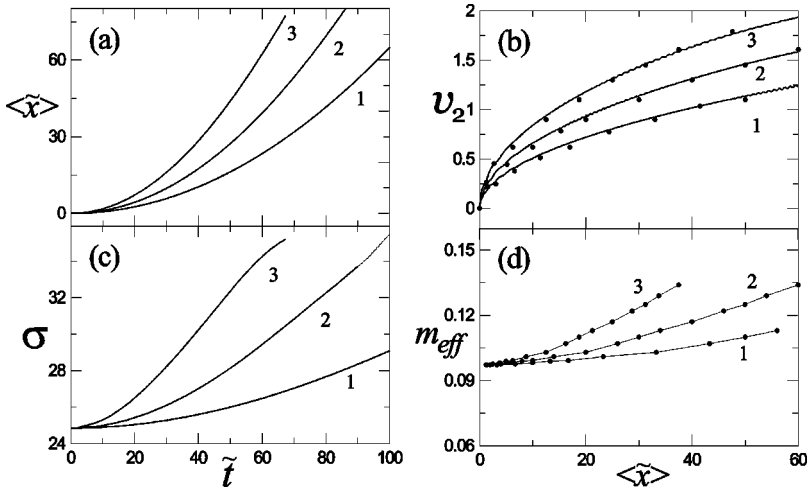

FIG. 2. (a) The coordinate of the soliton center of mass, $\langle\tilde{x}\rangle$, vs time. (b) Dependences of the carrier wave group velocity v_2 obtained directly from the periodic structure (dots) and velocity of the soliton center of mass obtained from direct numerical simulations (solid line). (c) Evolution of the dispersion of the soliton. (d) Dependence of the effective mass m_2 on the soliton coordinate. Curves 1, 2, and 3 correspond to $\epsilon = 0.02, 0.03$, and 0.04.

eration [see Fig. 2(b)]. An example of the dynamics of the coordinate of the condensate center of mass, $\langle\tilde{x}\rangle$, and its dispersion $\sigma=(\langle\tilde{x}^2\rangle-\langle\tilde{x}\rangle^2)^{1/2}$ obtained by numerical integration of Eq. (3) are shown in Figs. 2(a) and 2(c) (angular brackets stand for the spatial average). From this figure one can see that the soliton indeed undergoes acceleration in such a way that the soliton velocity follows the change of the group velocity of the background. Simultaneously, the dispersion of the soliton increases as is shown in Fig. 2(c). At first sight this result does not resemble the model given by Eq. (5) because according to this model the soliton width should decrease as the effective mass increases.

In order to explain the apparent discrepancy, let us consider the dispersion relation of the second zone $\mathcal{E}_2(k)$ in the vicinity of the band edge in more detail. Since $\mathcal{E}_2(k)$ is an even function of the wave vector, one can expand

$$\mathcal{E}_2(k) = \mathcal{E}^{(2)} + \frac{1}{2}\partial_k^2\mathcal{E}_2(k_0)(k-k_0)^2 + \frac{1}{4!}\partial_k^4\mathcal{E}_2(k_0)(k-k_0)^4, \tag{8}$$

where $\mathcal{E}^{(2)}=\mathcal{E}_2(k_0)$. We assume that (i) the center of soliton is displaced from the point $\tilde{x}=0$, where its energy was $\mathcal{E}_2$, to some point $\tilde{x}=\tilde{X}$ without change of energy, and (ii) the gap is large enough that within the range $0<\tilde{x}<\tilde{X}$ in the leading order one can neglect the change of the functional dependence of $\mathcal{E}_2$ on the wave vector k. Then one has the situation illustrated in Fig. 3. When the soliton moves from $\tilde{x}=0$ to $\tilde{x}=\tilde{X}$, the acquired energy shift $\Delta\mathcal{E}$ toward the allowed zone can be estimated as $\beta\tilde{X}$, where β is a small ($\beta\ll 1$) angle between the slope of the band gap edge and the x axis corresponding to the energy $\mathcal{E}_2$ (see the left figure in Fig. 3). The same energy shift on the diagram $\mathcal{E}_2(k)$, giving the energy $\mathcal{E}^{(2)}+\Delta\mathcal{E}$, corresponds to the wave vector k_1, which can be approximately found from the equation $(k_1-k_0)^2=2m_2\Delta\mathcal{E}$: $k_1=k_0+\sqrt{2m_2\beta\tilde{X}}$. Hence, one finds that the dependence of the group velocity on the coordinate $\tilde{x}$ is given by

$$v_2 = \begin{cases} \sqrt{\dfrac{2\beta\tilde{x}}{m_2}}, & \tilde{x}>0, \\ 0, & \tilde{x}\leqslant 0, \end{cases} \tag{9}$$

while the dependence of the effective mass is approximated by

$$m_2(\tilde{x}) = m_{20} - m_{20}^2\tilde{x}^2\Delta m, \quad \Delta m = \frac{\beta}{6}m_{20}\partial_k^4\mathcal{E}_2(k_0), \tag{10}$$

where m_{20} is the effective mass at the boundary of the zone, i.e., at $\tilde{x}=0$ [notice that it follows from Fig. 2(d) that $\partial_k^4\mathcal{E}_2(k_0)<0$].

It is remarkable that the above simplified estimates yield rather precise estimates for the relevant quantities. Indeed, for $\epsilon=0.02$ from Fig. 1(d) and Fig. 2(d) one obtains $\beta\approx 0.0013$ and $m_2\approx 0.1$, which gives for $\tilde{X}=30$ an estimate of $v_2(\tilde{X}=30)\approx 0.88$, in accordance with Eq. (9), while the numerical value is $v_2(\tilde{X}=30)\approx 0.87$ [see Fig. 2(b)].

Returning to the soliton dynamics shown in Figs. 1 and 2, let us neglect the small change of the effective mass, i.e., make the substitution $m_\alpha=m_{\alpha 0}$ in the equation for slowly varying amplitude (1), and compute the following integral identities:

$$\frac{dN}{dT} = \int_{-\infty}^{\infty}(v_\alpha)_X|\Psi|^2dX, \tag{11}$$

$$\frac{dP}{dT} = 0, P = -i\int_{-\infty}^{\infty}\overline{\Psi}\Psi_X dX, \tag{12}$$

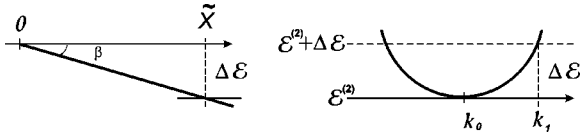

FIG. 3. Schematic illustration of the calculus of the dependence of the group velocity and the effective mass on the coordinate, for a linearly modulated potential. The notations are defined in the text.

$$\frac{d\langle X^2\rangle}{dT} = \frac{i}{m}\int_{-\infty}^{\infty} X(\bar{\Psi}_X\Psi - \bar{\Psi}\Psi_X)dX + \int_{-\infty}^{\infty}(X^2 v_\alpha)_X|\Psi|^2 dX, \quad \langle X^2\rangle = \int_{-\infty}^{\infty} X^2|\Psi|^2 dX, \tag{13}$$

where N is the number of particles given by Eq. (6), P is the wave momentum in the frame moving with the group velocity of the carrier wave, and $\sqrt{\langle X^2\rangle/N}$ is the average width of the wave packet. Then it follows from Eq. (13) that the total momentum is preserved. Moreover, for the soliton ansatz (5) it is zero, which reflects the fact that the condensate is moving with the group velocity of the carrier wave, corroborating the findings shown in Fig. 2(b). From Eq. (11) it follows that the number of particles is not preserved. This, however, does not contradict the conservation law of the total number of atoms in the Gross-Pitaevskii equation since the model given by Eq. (1) describes the main approximation of the ground state and does not account for high-frequency radiation while, on the other hand, in the leading order, the soliton is moving in the inhomogeneous medium and thus represents a radiating matter wave [14]. Considering the second band, $\alpha=2$, and approximating the solution by Eqs. (5) and (9), one can rewrite Eq. (11) as

$$\frac{dN}{dT} = \sqrt{\frac{\beta}{2m_{20}}}\int_0^{\infty}\frac{dX}{\sqrt{X}}[|\Psi_s(X,T)|^2 - |\Psi_s(0,T)|^2] \leqslant 0,$$

which reflects the fact that the soliton loses particles. Finally, taking into account that Ψ_s given by Eq. (5) is real, one obtains from Eq. (13)

$$\frac{d\langle X^2\rangle}{dT} = 5\sqrt{\frac{\beta}{2m_{20}}}\int_0^{\infty} X^{3/2}|\Psi_s(X,T)|^2 dX > 0,$$

which means an increase of the soliton width, as observed in Figs. 1(c) and 2(c).

The wave packet during its motion follows the carrier wave and thus rapidly acquires a relatively large group velocity which is of the order of unity. The latter factor does not allow adiabatic adjustment of the soliton parameters to increase the effective mass of the carrier wave [see Eq. (10) and Fig. 1(d)]. Nonadiabaticity of the process manifests itself in radiative losses and broadening of the wave packet. This process continues as the soliton moves to the region with small potential depth, as observed in Fig. 1(c), and with time, as a matter of fact, the wave loses its solitonic properties, transforming itself into a dispersive wave packet. It is worth pointing out that another simple way to look at the broadening of the wave packet is to take into account that the soliton wave front has a larger velocity than the tail and this leads to spreading of the pulse.

IV. OSCILLATION OF THE MATTER WAVE IN A LATTICE SUBJECT TO PARABOLIC MODULATION

Let us consider now a soliton dynamics [the initial profile is shown in Fig. 4(b)] in a lattice modulated by a parabolic function [see Fig. 4(a)]

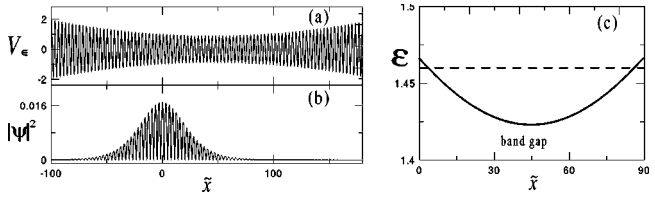

FIG. 4. (a) The inhomogeneous periodic potential V_ϵ given by Eq. (14) with $\epsilon=0.02$ and $\Delta\tilde{x}=45$. (b) The initial profile of an envelope soliton [the same as in Fig. 1(a)]. (c) The upper edge of the first band gap for the potential shown in (a).

$$V_\epsilon(\tilde{x}) = [1 + \epsilon^{5/2}(\tilde{x} - \Delta\tilde{x})^2]\cos(2\tilde{x}) \tag{14}$$

where $\Delta\tilde{x}$ is introduced for the initial relative shift between the soliton center and the minimum of the parabolic modulation. The upper bound of the first gap of this potential for $\epsilon=0.02$ is depicted in Fig. 4(c).

Now one observes oscillations of the condensate cloud (see Fig. 5). The accelerating part of this motion when the soliton is moving toward the center of the potential is explained in the previous section. After passing the central part of the potential, the soliton is decelerating and at some point the velocity of the center of mass of the cloud becomes zero. This occurs in the vicinity of the turning point x_{turn}, where the energy of the soliton falls into the forbidden gap [the intersections of dashed and solid lines in Fig. 4(c)]. In fact, in considering a soliton moving from the right to the left near the turning point, one can approximate the potential modulation by a linear function. Then, by using Eq. (9), the velocity of the background, and hence the velocity of the soliton, tends to zero as $\sqrt{x-x_{turn}}$, when the coordinate of the soliton center approaches the turning point. Thus one can speak about Bragg reflection of the soliton from an inhomogeneous periodic potential.

There are two features of the soliton dynamics to point out in this case. First, in contrast to the case of linear modu-

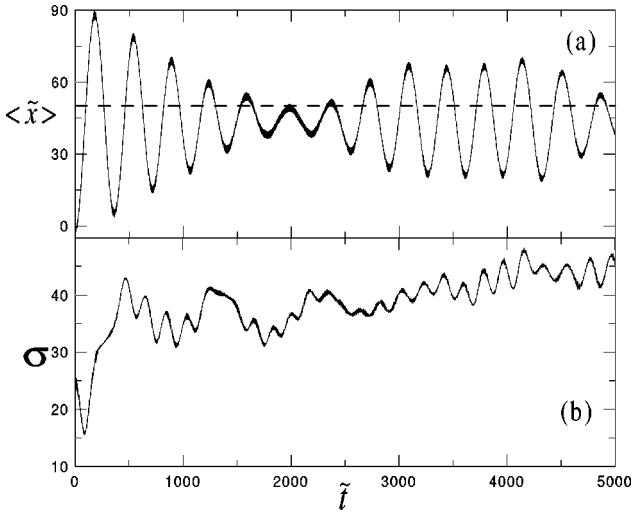

FIG. 5. Dynamics of the center of mass (a) and of dispersion (b) of the matter soliton. Parameters are the same as in Fig. 4 . The dashed line corresponds to $\langle\tilde{x}\rangle=\Delta\tilde{x}$.

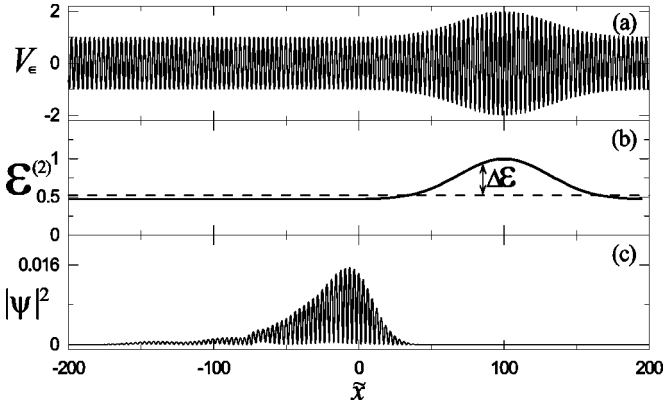

FIG. 6. (a) The lattice defect given by Eq. (15) with $\epsilon=0.05$ and $\Delta\tilde{x}=100$. (b) The upper edge of the lowest gap (solid line) and the energy of the soliton with the initial velocity $v=0.1$ (dashed line). Intersections of these lines represent the turning points. (c) Profile of the reflected soliton at time $t=150$. The initial soliton profile is the same as in Fig. 1(b).

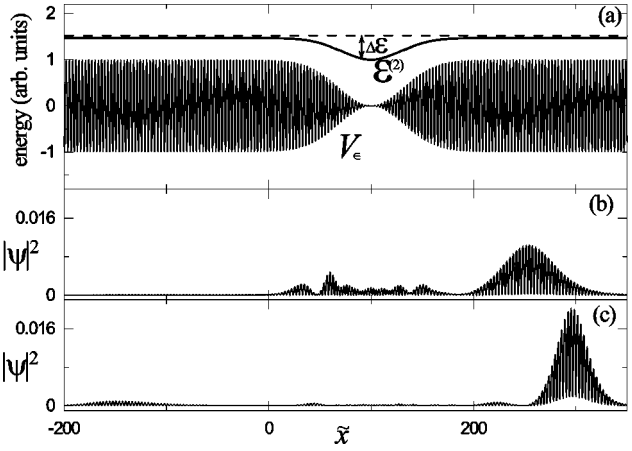

FIG. 7. (a) Periodic potential with the defect given by Eq. (16) and corresponding upper edge $\mathcal{E}^{(2)}$ of the first band gap (here the dashed line is the initial soliton energy). Parameters of the defect are $\epsilon=0.05$ and $\Delta\tilde{x}=100$. Profiles of the soliton with different initial velocities $v=0.1$ (b) and $v=0.3$ (c) at times $t=300$ and $t=190$, respectively. The initial soliton profile is the same as in Fig. 6 .

lation, in the initial stages the dispersion decreases [see Fig. 5(b)]. This compression of the pulse is explained by its large extension; when the leading part of the wave packet undergoes Bragg reflection and moves in the negative direction while the soliton center still moves in the positive direction. The second feature demonstrated in Fig. 5(a) is the appearance of a smaller frequency modulating the amplitude of oscillations of the wave packet. Assuming that the solution can be described approximately by the formula (5) where the coordinate of the soliton center $X_0(T)$ depends periodically on time with the effective linear oscillator frequency ν associated with the effective parabolic potential, we estimate it as $\nu=2\epsilon^{5/4}$ (≈ 0.014 in our simulations). This frequency approximately coincides with the higher frequency that can be seen in Fig. 5(a), which is ~ 0.017. The observed discrepancy is due to the fact that one is dealing with a modulated periodic potential, rather than with a real parabolic one. On the other hand, the envelope soliton is characterized by the internal frequency $\omega_{int}=m_2N^2/8$ [see Eq. (5)]. In our numerical simulations it is a low frequency $\omega_{int}\approx 0.002$. Thus the relation between the frequencies is $\omega_{int}/\nu\approx 8.6$, which corresponds to nine fast oscillations per one period of the slow modulation observed in Fig. 5(a).

V. INTERACTION OF A SOLITON WITH A DEFECT

The phenomenon of the Bragg reflection of a soliton can be directly observed in a system where the optical lattice has a local increase of depth, as shown in Fig. 6(a):

$$V_\epsilon(\tilde{x}) = [1 + e^{-\epsilon^{5/2}(\tilde{x}-\Delta\tilde{x})^2}]\cos(2\tilde{x}). \tag{15}$$

Local deformations of an optical lattice will be referred to as lattice defects. In this case, as before, we also start with a numerically obtained bright soliton, but add now some initial velocity v with respect to the stationary background, which is introduced by means of the phase factor $\psi(\tilde{x},0)e^{iv\tilde{x}/2}$. We are interested in the scattering process at different initial velocities, which are assumed to be small enough: $v \ll 1$.

In this case solitons are reflected from the defect [see the snapshot Fig. 6(c)]. This is the effect of the Bragg reflection, which is explained in Fig. 6(b). Indeed, due to increase of the lattice depth, the gap is also increased locally. That is why the soliton, which was initially moving with a relatively small group velocity v, at some point reaches the (curved) band edge [it is given by the intersection of dashed and solid lines in Fig. 6(b)] which prevents further propagation of the carrier wave. Thus, the defect described by Eq. (15) can be classified as repulsive.

Let us consider now the opposite situation, when the depth of the periodic potential is locally decreased [see Fig. 7(a)]:

$$V_\epsilon(\tilde{x}) = [1 - e^{-\epsilon^{5/2}(\tilde{x}-\Delta\tilde{x})^2}]\cos(2\tilde{x}), \tag{16}$$

what leads to local narrowing of the forbidden gap.

By using the arguments based on the band gap structure outlined below one may argue that the modulation described by Eq. (16) acts as an attractive impurity. Indeed, in the region of the defect there exists a shrinking of the forbidden band. Assuming as before that the soliton energy $\mathcal{E}$ is constant, one concludes that in the region of the defect the energy shift $\Delta\mathcal{E}$ (see Fig. 3) toward the allowed zone depends on the coordinate $\Delta\mathcal{E}=\Delta\mathcal{E}(\tilde{x})$: it increases as the soliton approaches the center of the defect and then decreases as the coordinate increases. Since larger $\Delta\mathcal{E}(\tilde{x})$ corresponds to larger velocities of the carrier wave, the soliton is accelerating when it approaches the defect and decelerating when it moves away from the defect.

Since the lattice modulation (16) acts as attractive, a number of atoms could be captured by such a defect, in the case when the initial kinetic energy of the condensate is small enough. This is exactly what we observe in the numerical simulations shown in Fig. 7(b). The higher-velocity matter waves pass through the defect without substantial change [see Fig. 7(b)].

VI. CONCLUSION

In conclusion, we have shown that in smoothly modulated optical lattices that can be created by using quasimonochromatic laser beams one can effectively manage matter solitons as they accelerate, decelerate, oscillate, or undergo reflection depending on the type of modulation imposed. Since the above processes are controlled by the periodic structure, not only one dynamical but also other properties of matter waves such as the energy, the effective mass, and the width of the soliton can be manipulated. Although in a particular dynamical process a matter wave can lose its solitonic properties, the effective mass approximation provides a qualitative explanation of the main features of the soliton dynamics, if the wave packet possesses a substantially larger extension than the lattice period and the lattice modulations are smooth enough.

ACKNOWLEDGMENTS

The work of V.A.B. has been supported by the FCT Grant No. SFRH/BPD/5632/2001. V.V.K. acknowledges support from the European Grant COSYC No. HPRN-CT-2000-00158. V.K. acknowledges support from COST P11 Action. Cooperative work was supported by the bilateral agreement GRICES/Czech Academy of Sciences.

[1] B. P. Anderson and M. A. Kasevich, Science **282**, 1686 (1998).

[2] F. S. Cataliotti, S. Burger, C. Fort, P. Maddaloni, F. Minardi, A. Trombettoni, A. Smerzi, and M. Inguscio, Science **293**, 843 (2001); M. Greiner, I. Bloch, O. Mandel, T. W. Hänsch, and T. Esslinger, Phys. Rev. Lett. **87**, 160405 (2002); M. Greiner, O. Mandel, T. Esslinger, T. W. Hänsch, and I. Bloch, Nature (London) **415**, 39 (2002); M. Krämer, L. Pitaevskii, and S. Stringari, Phys. Rev. Lett. **88**, 180404 (2002).

[3] L. Fallani, L. De Sarlo, J. E. Lye, M. Modugno, R. Saers, C. Fort, and M. Inguscio, e-print cond-mat/0404045.

[4] See, e.g., V. V. Konotop and M. Salerno, Phys. Rev. A **65**, 021602(R) (2002), and references therein.

[5] See, e.g., M. Cristiani, O. Morsch, J. H. Müller, D. Ciampini, and E. Arimondo, Phys. Rev. A **65**, 063612 (2002), and references therein.

[6] M. Jona-Lasinio *et al.*, Phys. Rev. Lett. **91**, 230406 (2003).

[7] O. Morsch, J. H. Müller, M. Cristiani, D. Ciampini, and E. Arimondo, Phys. Rev. Lett. **87**, 140402 (2001).

[8] L. Fallani, F. S. Cataliotti, J. Catani, C. Fort, M. Modugno, M. Zawada, and M. Inguscio, Phys. Rev. Lett. **91**, 240405 (2003).

[9] B. Eiermann, P. Treutlein, Th. Anker, M. Albiez, M. Taglieber, K.-P. Marzlin, and M. K. Oberthaler, Phys. Rev. Lett. **91**, 060402 (2003).

[10] R. G. Scott, A. M. Martin, T. M. Fromhold, S. Bujkiewicz, F. W. Sheard, and M. Leadbeater, Phys. Rev. Lett. **90**, 110404 (2003).

[11] I. Carusotto, D. Embriaco, and G. C. La Rocca, Phys. Rev. A **65**, 053611 (2002).

[12] B. Eiermann, Th. Anker, M. Albiez, M. Taglieber, P. Treutlein, K. P. Marzlin, and M. K. Oberthaler, Phys. Rev. Lett. **92**, 230401 (2004).

[13] G. L. Alfimov, V. V. Konotop, and M. Salerno, Europhys. Lett. **58**, 7 (2002).

[14] Recently, radiative losses of a matter soliton in an optical lattice were considered by A. V. Yulin, D. V. Skryabin, and P. St. J. Russell, Phys. Rev. Lett. **91**, 260402 (2003).